

# MECHANICAL DESIGN OF NSLS X-25 SMALL GAP UNDULATOR

D. Lynch, G. Rakowsky

BNL, Upton, NY 11973, USA

Phone: 631-344-2253, FAX: 631-344-3238

e-mail: dlynch@bnl.gov

## Abstract

*The mechanical design considerations are discussed with respect to the X-25 small gap in-vacuum hybrid permanent magnet and vanadium permendur undulator, currently under design at the NSLS. Performance predictions, mechanical, thermal and structural design methodology, both common to undulators of this type, and unique to the subject undulator, are discussed. The design requirements and mechanical difficulties for holding, positioning and driving the magnetic arrays are examined. Structural, thermal and electrical considerations which influenced the design are then analysed. Novel design concepts being considered for this undulator to improve performance and deal with design constraints unique to this application are also explored. This undulator will replace an existing permanent magnet wiggler currently in service at X-25.*

## 1. Introduction

Beginning with the Prototype Small Gap Undulator (PSGU), installed in the NSLS x-ray storage ring in 1994, and continuing to the present, the NSLS has developed a series of small gap undulator insertion devices for high brightness and high flux. The benefits of such devices has been well documented by Stefan[1]. The undulator described in this report is the latest in this series of devices and will build on the successful mechanical design concepts proven in the earlier devices, and will additionally incorporate some new features to improve on previous designs.

The MGU design, as has been documented by Lynch[2], was the most recent successful effort in the NSLS undulator development, with the initial deployment at NSLS X-13 in December of 2001. This version has been successfully operating and serving a variety of scientific disciplines at the NSLS[3]. A second version of the MGU, modified to fit in a smaller longitudinal space between 2 RF cavities in the NSLS x-ray ring was recently successfully commissioned to serve a biology beamline at X-29.

The X-25 undulator, dubbed "MGU-25", currently in design at the NSLS, will utilize many of the mechanical features of the MGU, including the magnet array positioning and holding scheme, RF continuity inlet and outlet transitions and vacuum monitoring and conditioning scheme. Due to the length of the undulator, the undulator base, vacuum chamber and magnet drive system require a different strategy from the MGU. The strategies for testing and assembly of MGU-25 will also require new approaches. These items will be described in this paper.

This new in-vacuum undulator will soon replace the 15-year old X25 Wiggler in the NSLS X-ray Ring. It will provide a high-brightness, tunable x-ray source over the photon range of 1.9-20 keV, with continuous coverage in overlapping bands, utilizing the fundamental, 2<sup>nd</sup>, 3<sup>rd</sup>, 5<sup>th</sup>, 7<sup>th</sup> and 9<sup>th</sup> harmonics. Unlike newer, low-emittance, "third-generation" light sources, there is a significant and usable 2<sup>nd</sup> harmonic on-axis due to the rather large emittance of the 2.8 GeV electron beam. The tuning range of the 2<sup>nd</sup> harmonic fills the gap between the top of the 2:1 tuning range of the fundamental (1.9-3.8 keV) and the bottom of the 3<sup>rd</sup> harmonic's range (5.7 keV). MGU-25 will deliver to the Protein Crystallography program on the X25 beamline between 30 times and 2 times brighter x-ray beams over its entire tuning range, compared to the old X25 Wiggler.

## 2. Undulator Magnet Design

The magnet arrays of MGU-25 will be approximately 1 m long, with parameters given in Table 1. The pole material is Vanadium Permendur, chosen for its very high saturation flux density ( $B_{\text{sat}} = 2.3 \text{ T}$ ). The expected performance is predicated on use of the new 44AH grade of NdFeB permanent magnet material (Sumitomo Special Metals), which offers a combination of very high remanent field ( $B_r \geq 1.3 \text{ T}$ ) and very high intrinsic coercivity ( $H_{\text{ci}} \geq 22 \text{ kOe}$ ). The high  $H_{\text{ci}}$  value is the same as for the 39SH grade used in our previous successful mini-gap undulators MGU-13 and MGU-29, and will permit baking of the magnet arrays up to  $100^\circ\text{C}$  without loss of magnetization.

Table 1. MGU-25 Parameters

|                           |             |     |
|---------------------------|-------------|-----|
| Length                    | 1.02        | m   |
| Period                    | 18          | mm  |
| No. full-strength periods | 55          |     |
| Gap range                 | 5.6 – 11.25 | mm  |
| Peak Field                | 0.9 – 0.3   | T   |
| K                         | 1.5 – 0.5   |     |
| Electron energy           | 2.8         | GeV |
| E(fundamental)            | 1.9 – 3.7   | keV |
| E(2 <sup>nd</sup> harm.)  | 3.8 – 7.4   | keV |
| E(3 <sup>rd</sup> harm.)  | 5.8 – 11    | keV |
| E(5 <sup>th</sup> harm.)  | 9.6 – 18    | keV |
| E(7 <sup>th</sup> harm.)  | 13.5 – 26   | keV |
| E(9 <sup>th</sup> harm.)  | 17.3 – 33   | keV |

Figure 1 is an isometric rendering of the MGU magnet arrays by the 3D magnetic modeling code Radia (available from ESRF at [www.esrf.fr](http://www.esrf.fr).) Only the first few periods are shown, so that the end design can be seen more clearly.

Poles and magnets have the following dimensions:

### POLES

Main Poles: 40.0 x 24.00 x 3.00 mm  
Pole #2: 40.0 x 23.50 x 3.00 mm  
Pole #4: 40.0 x 23.975 x 3.00 mm

Long edges of pole tips chamfered 0.50 x 0.50 mm

### MAGNETS

Main Magnets: 49.0 x 28.50 x 5.90 mm  
End magnet heights (% of main magnet height):  
#1: 19.3% (only 2 corners chamfered)  
#2: 55.1%  
#3: 82.1%  
Corners chamfered 3.0 x 3.0 mm (45°)

Magnets are recessed 0.25 mm below poletips.

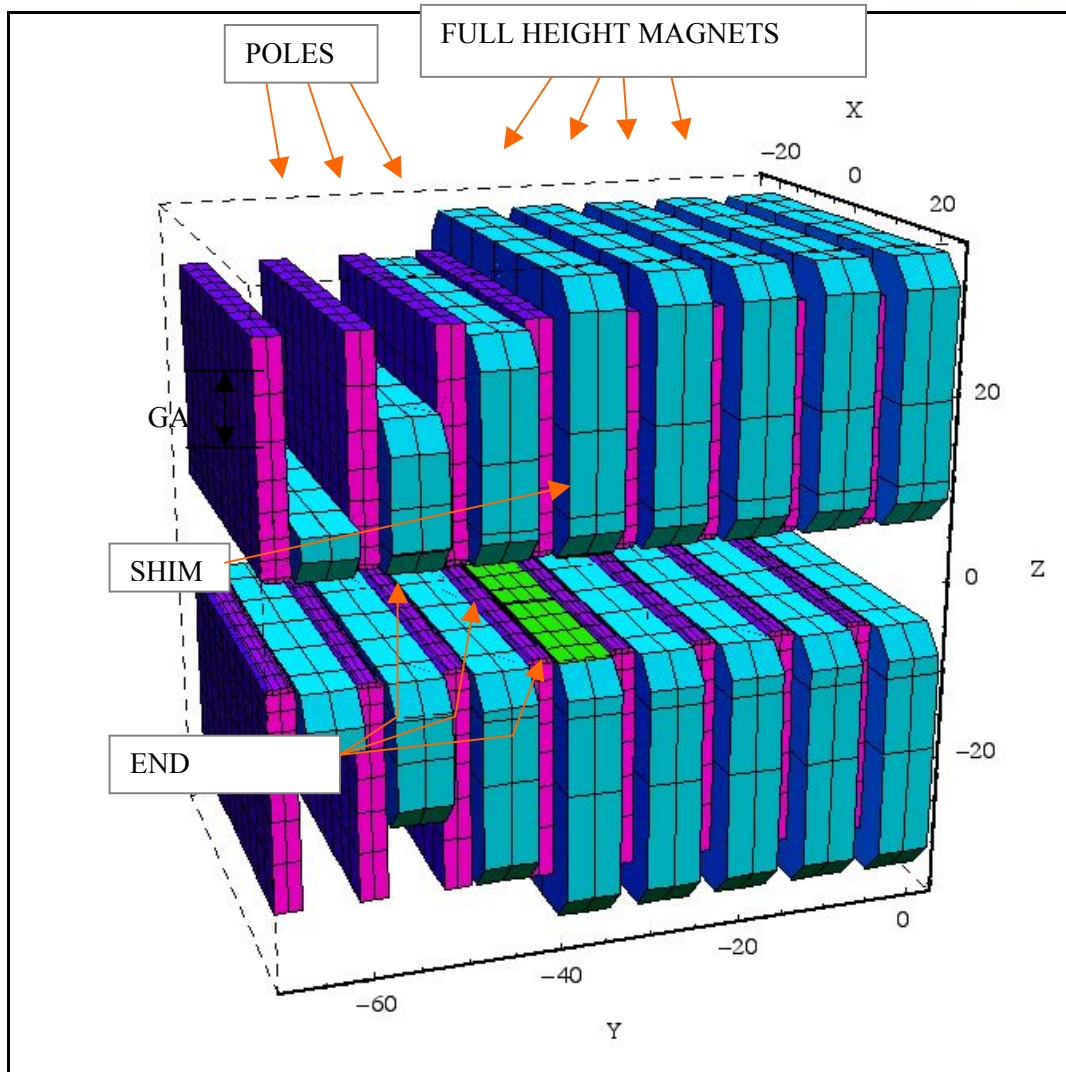


Figure 1. Magnet arrays of MGU-25. Only the first few periods are shown for clarity.

The first three magnets from each end are graduated in height to provide an optimal taper of the field amplitude as the electron enters and exits the structure. In addition, the 2<sup>nd</sup> and 4<sup>th</sup> poles are reduced in height by 0.5 and 0.025 mm respectively (i.e., locally increasing the gap by 1.00 mm at pole #2, and by 0.05 mm at pole #4.) Finally, a steel shim 0.25 mm thick is placed on the face of the 4<sup>th</sup> magnet from each end to fine-tune the trajectory. In the ideal case with no errors, this termination design optimizes the electron trajectory over the full range of operating gaps (5.6 to 11.25 mm) as follows:

- Achieves zero net orbit displacement between entry and exit;
- The axis of the sinusoidal part of the trajectory is centered relative to the reference orbit (the orbit without the undulator);
- The angle of the axis of the sinusoidal part of the trajectory relative to the reference orbit is  $< 1$  microradian.
- Maximizes the number of poles contributing to the resonant output.

Result (i) minimizes horizontal emittance growth due to orbit displacement.

Results (ii) and (iii) assure that the radiated photon beam is tangent to the electron orbit.

The structure has an even number of poles, so the field is “anti-symmetric” about the midpoint. By this symmetry any inherent steering errors due to the terminations are of opposite sign, automatically assuring zero net steering error.

The undulator was modeled with only 4 full periods to limit the size of the problem and the running time, yet it is long enough so that the central part of the undulator field and trajectory are developed free of end effects. The field and trajectory computed from the model are plotted in Figure 2 for gaps of (a) 5.6 mm and (b) 11.25 mm. The trajectory is calculated by a particle tracking Runge-Kutta routine. The particle is launched with zero offset and angle ( $x = 0, x' = 0$ ) and its position and angle are calculated every 0.6 mm (30 points per period). We can see that the termination design results in the trajectory exiting with essentially zero offset and angle, and the main part of the trajectory is parallel and centered about the axis. This assures that the photon beam is also parallel to the axis. This condition is well preserved over the full gap tuning range. (Results at intermediate gaps are similar, but are not shown.) Finally, the end design produces a trajectory having very nearly full amplitude by the third pole, maximizing the number of poles radiating in-phase and contributing to the resonant output.

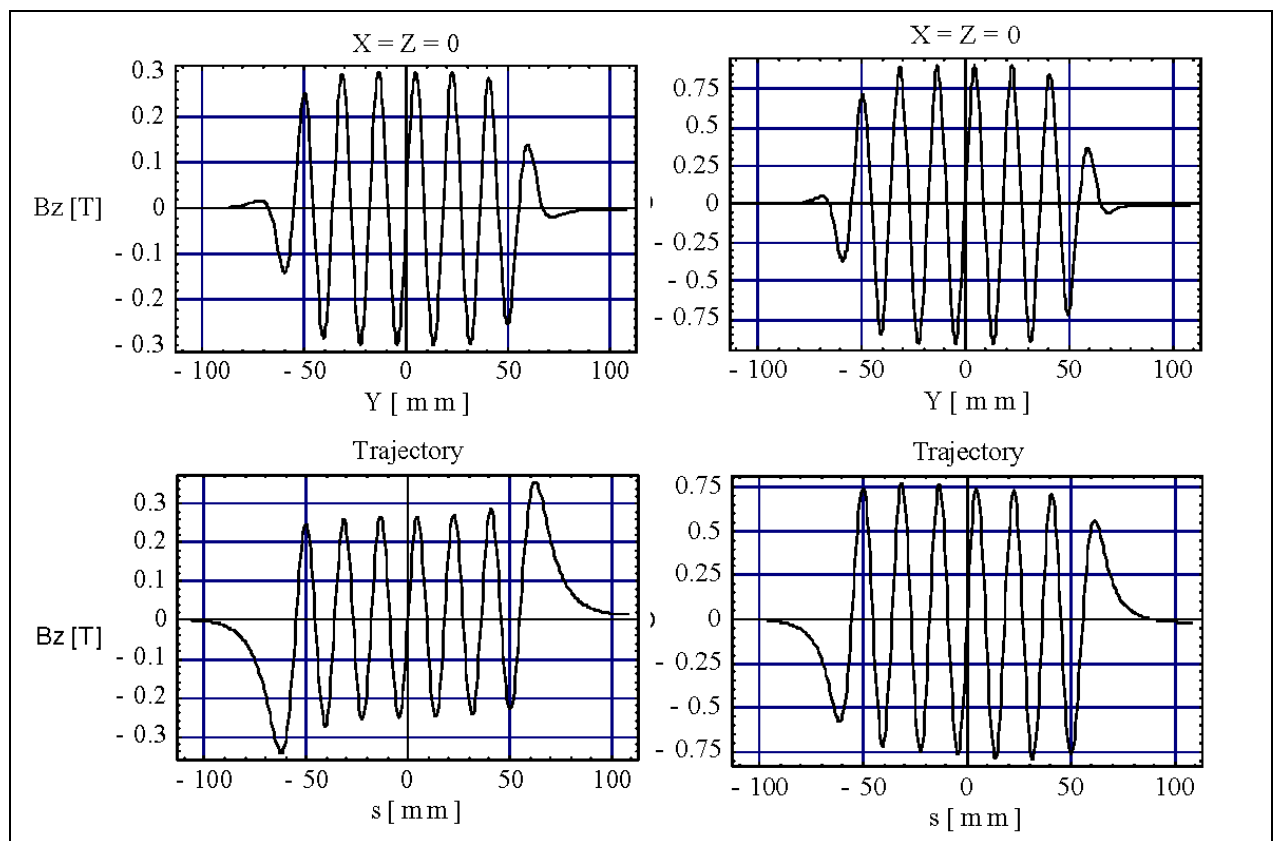


Figure 2. Field and trajectory plots for the 4-period model for

(a) minimum gap (5.6 mm) and

(b) maximum operating gap (11.25 mm).

The maximum gap of 11.25 mm represents the gap where the K-value equals 0.5, which is generally considered as the minimum value, below which optical output falls off too rapidly to be useful. Nevertheless, the mechanical travel of the gap separation mechanism will allow the gap to be opened considerably more than 11.25 mm to allow the undulator field to fall to a negligibly small enough value to be essentially “invisible” to the electron beam. Undulator

peak field decreases exponentially with increasing gap, so doubling the gap to 22.5 mm, for example, will reduce the field by about a factor of 7 to 0.04 T. As the gap is opened beyond 11.25 mm, the optimized end conditions are preserved quite well.

The fields and trajectories computed from the model assume zero mechanical errors and uniform magnetic properties. Of course, random errors are always present due to mechanical tolerances and variations in magnet strength. Critical tolerances will be controlled in manufacturing and inspection. Magnets will first be individually measured, then sorted and paired to balance variations in magnet strength to first order. Remaining mechanical and magnetic errors cause random, local trajectory and phase errors which will be identified during field measurements of the assembled structure and will be corrected by various means, collectively referred to as “shimming”.

An especially powerful diagnostic is “phase error”, computed from the cumulative difference of trajectory path length between the actual and ideal trajectory. In addition to identifying random errors, phase error can reveal systematic errors, like gap taper and mechanical deformation of the arrays due to magnetic forces, with far greater sensitivity than mechanical measurement or optical survey. Phase error will be used to achieve final alignment of the arrays.

### 3. Mechanical Design

#### 3.1. Mechanical Requirements

In addition to the magnet array dimensional requirements, the MGU-25 device is required to meet the following design tolerances:

| Item                                   | Tolerance        |
|--|------------------|
| magnet/pole width                      | +/- 125 $\mu$ m  |
| magnet height                          | +/- 25 $\mu$ m   |
| magnet thickness                       | +/- 25 $\mu$ m   |
| pole height                            | +/- 50 $\mu$ m   |
| pole thickness                         | +/- 12 $\mu$ m   |
| pole-to-pole flatness                  | +/- 12 $\mu$ m   |
| period                                 | +/- 12 $\mu$ m   |
| magnet array pitch/yaw/roll (relative) | +/- 25 $\mu$ rad |
| magnet array pitch/yaw/roll (absolute) | +/- 25 $\mu$ rad |
| magnet array horizontal/vertical rack  | +/- 12 $\mu$ m   |
| gap control                            | +/- 12 $\mu$ m   |
| gap repeatability                      | +/- 12 $\mu$ m   |

#### 3.2. Magnet Drive

The magnet drive and magnet positioning system consists of a rigid main structure and 4 magnet arms moving along 4 rails with 2 stepper motor controlled drive screw mechanisms. One screw is for centering the magnets around the electron beam axis and the other for opening/closing the gap. The scheme for controlling the gap utilizes a single screw which then transfers load to 4 opposing wedges which transform a linear horizontal motion into an opening or closing motion of the 4 drive arms. This scheme eliminates the need for worm drives and left hand/right hand screw drives and allows for high precision coordination among

the 4 drive arms. These adjustments will be calibrated during magnet lab testing, and may be controlled remotely to allow for injection and tuning during operation. High precision recirculating ball bearing runner blocks and matching rails ensure high precision positional manipulation and repeatability.

There are 5 other sets of manual kinematic adjustments to allow x, y, z positional adjustment and pitch, roll and yaw angular adjustments. These adjustments will be on the base, the drive support structure, upper and lower drive arms and the vacuum chamber. The manual adjustments will be calibrated and set during magnet lab testing, then adjusted and permanently fixed during installation. The magnet drive scheme is shown in figure 3.

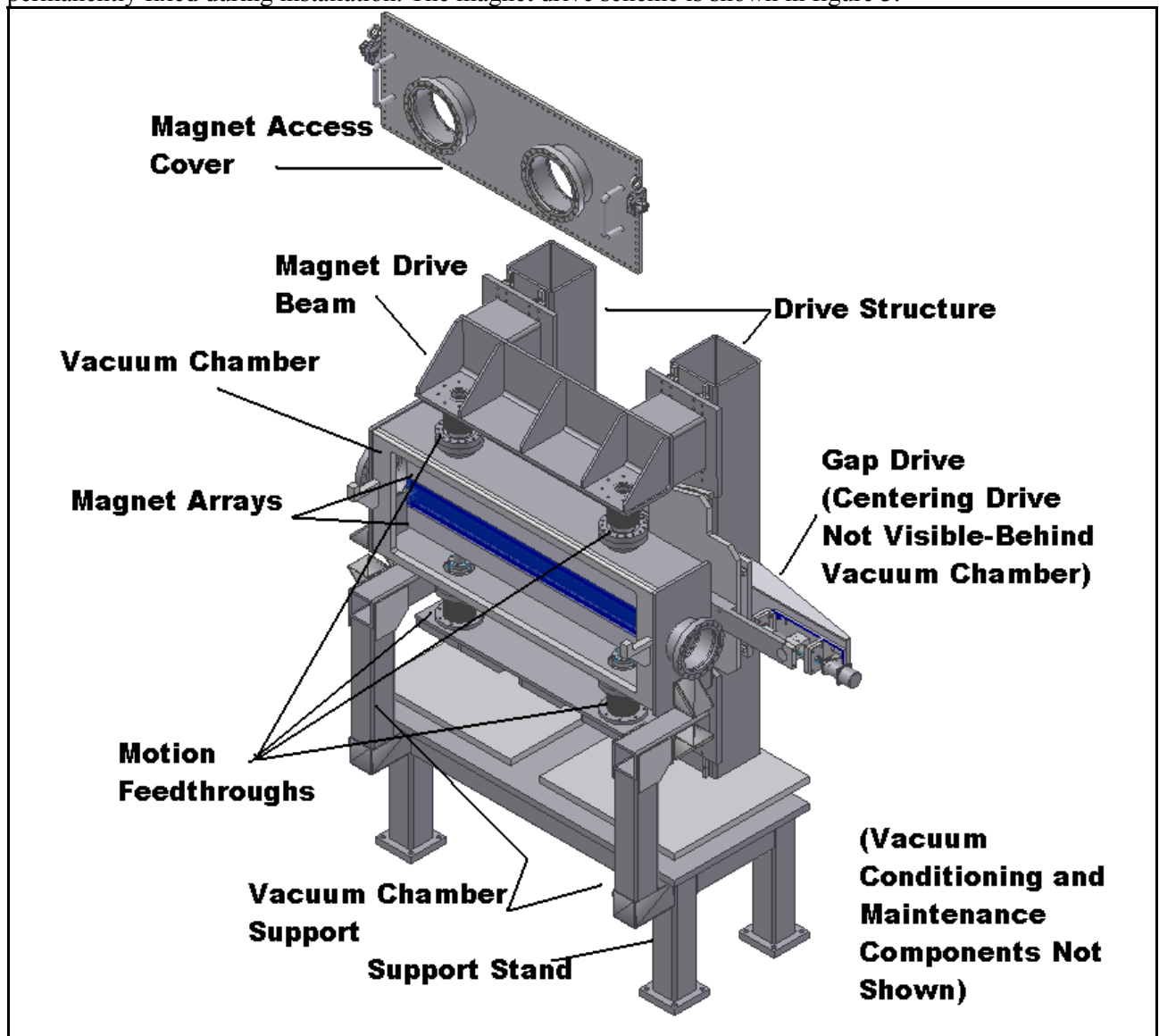


Figure3: Magnet Drive Schematic

### 3.3. Magnet Arrays

The X-25 undulator magnet arrays are similar in concept to those of the MGU, and the dimensions of the individual magnets and poles are not significantly different. The magnet positioning and holding concepts utilized for the MGU proved to be readily manufactured, reliably accurate, convenient to assemble, and structurally sound. The concept utilizes a single machined base with side rails machined with "fingers" to hold and separate poles and

magnets, The poles and magnets are then clamped in place with a series of small clips and screws. The X-25 undulator has a longer period and a greater number of periods, but the scheme utilized in the MGU is easily extended to handle these differences.

One of the difficulties with the design of high field small gap undulators is the attractive force between the two arrays. For the MGU this force is resisted by the structural design of the magnet drive. This approach will most likely be adopted for the X-25 undulator, although a novel scheme using a series of outboard opposing magnets sized to cancel the attractive force of the arrays is currently under consideration. It is uncertain at this point if such a scheme would negatively impact the undulator field quality, and as such additional analyses and prototyping will be necessary to see if this concept is practical. The design of the magnet drive structure will proceed under the assumption that the opposing magnets scheme will not be used, but with accommodation in the design of the vacuum chamber for the opposing magnets, should it be found practical. The magnet array positioning and holding design is shown in Figure 4.

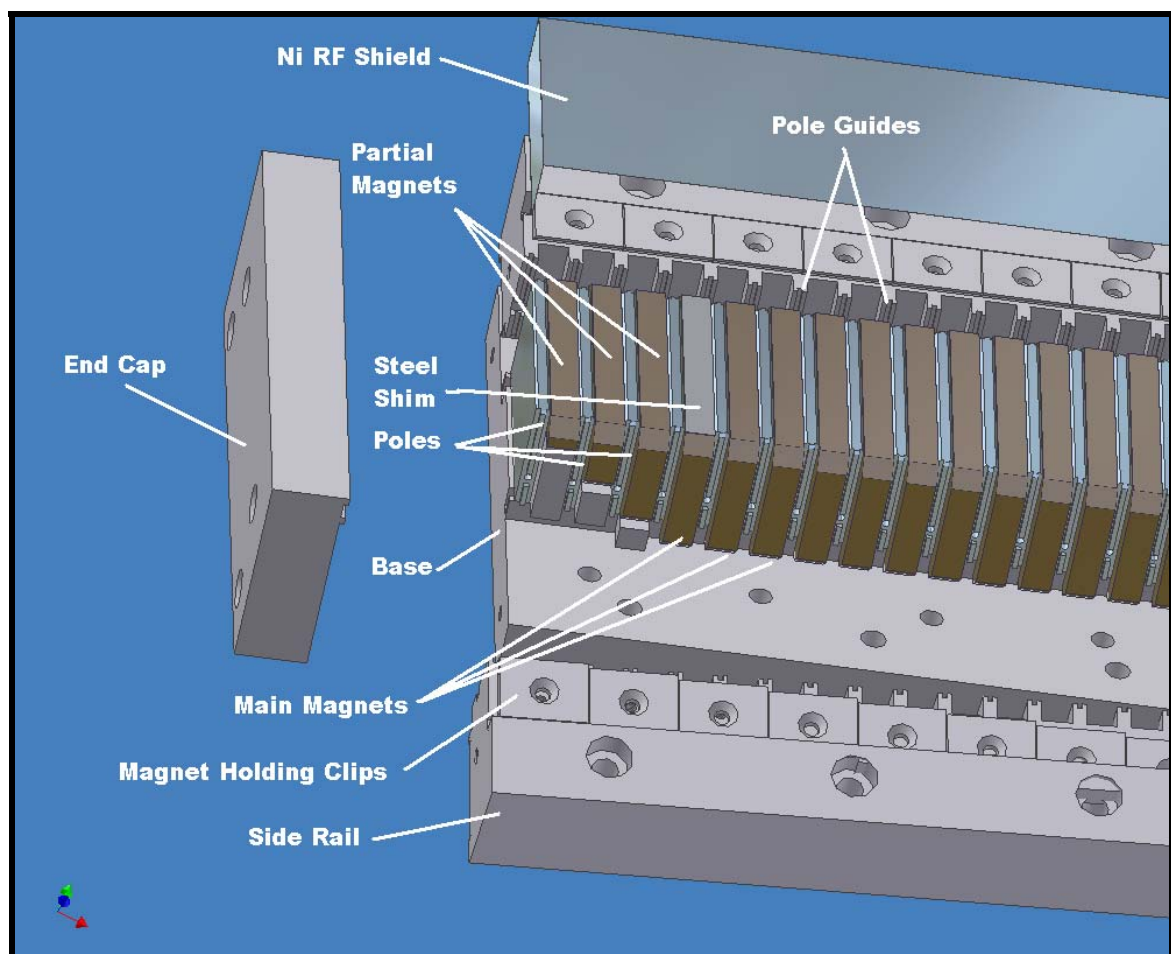


Figure 4: magnet array scheme

### 3.4. Vacuum Chamber and Magnet Assembly

The vacuum chamber design will be similar in concept to the original MGU design, except that the magnet arrays will be supported from 2 "arms" for the upper array and 2 arms for the lower array and the arrays will not be retractable out of the vacuum chamber. This then requires that either the arrays be tested and aligned after assembly into the vacuum chamber, or that a scheme be developed to test and align the arrays out of the vacuum chamber, then

insert the arrays axially into the chamber and replicate the alignment from the out-of-chamber tests.

The chamber design will also require a variety of ports for an ion pump, a getter pump, and RGA analyzer, a glow discharge cleaning assembly, ion gauge and bleed up ports, in addition to the electron beam ports and the magnet arm feedthrough ports. A schematic for the vacuum chamber is illustrated in figure 5.

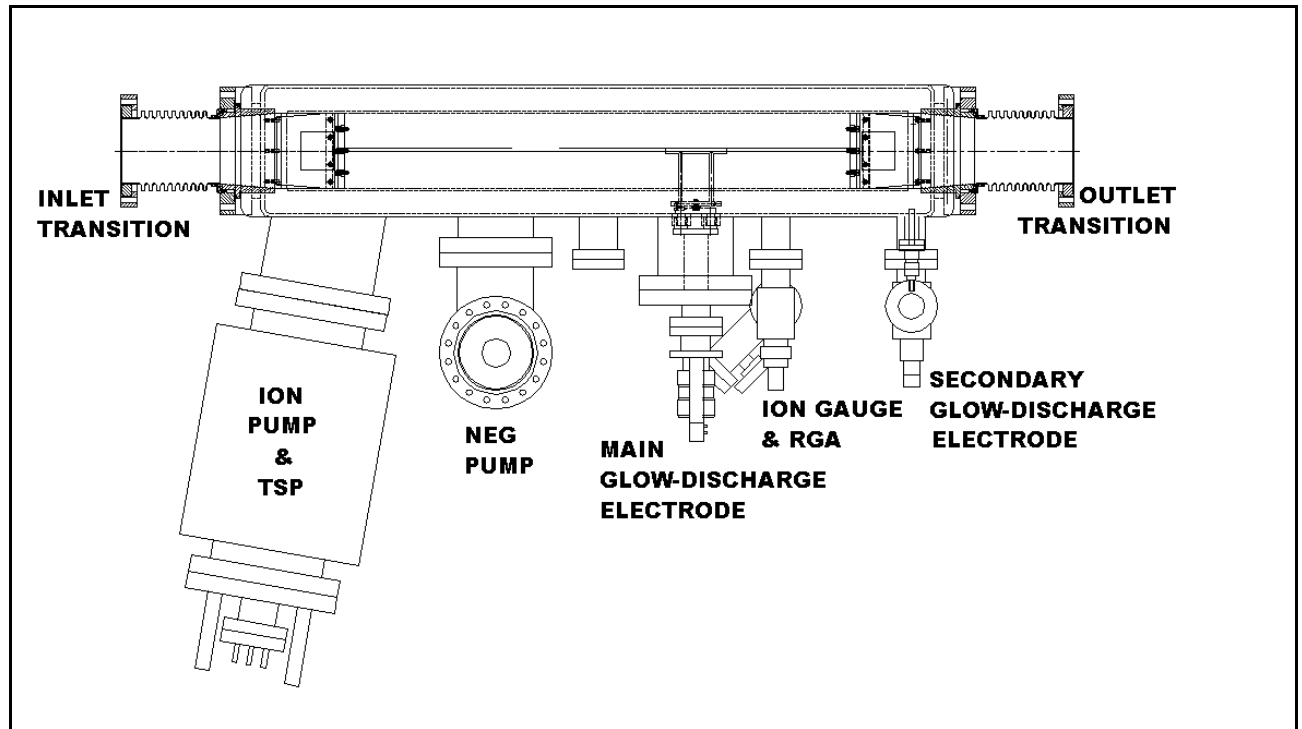


Figure 5: vacuum chamber schematic

### 3.5. Thermal Design

The MGU-25 undulator is unaffected by its own radiation but could be irradiated by the dipole magnet upstream, and may be subjected to some RF heating. A radiation absorber will be designed to protect uncooled surfaces of the vacuum chamber from dipole radiation. In addition, each magnet array will have a Nickel face sheet for RF continuity and the array base plate backing block will have integral cooling passages. These passages will serve the dual purpose of absorbing any operational heat loads and maintaining uniform magnet array temperatures. The remanent field of the magnet materials increases with decreasing magnet temperature. For this reason the cooling passages are being designed to accommodate either cooling water at about 20 °C or cooled N<sub>2</sub> gas at about -80°C. Cooling the nominal magnet temperatures 100°C will gain 10% (about 0.1 Tesla) in magnet field.

### 3.6. Transitions and RF Continuity

The MGU-25 vacuum space requires a smooth transition to the vertical transit space in the undulator chamber and RF electrical continuity for the image current (experience with previous in-vacuum undulators at the NSLS has demonstrated that the horizontal smoothness and continuity is not an issue). In previous NSLS undulators this has been accomplished with a fixed shape transition at the inlet and outlet with flexible thin sheets of copper to define the upper and lower surfaces of the variable beam space and to provide for electrical continuity.

Electrical continuity across the magnet array is provided by a 25 $\mu$ m Nickel shield which is held fast by the arrays magnetic field. This concept will be adopted for the MGU-25.

#### 4. Acknowledgements

The authors would like to acknowledge the efforts of Lonny Berman, Steve Hulbert, Paul Montanez and Florin Staicu all of the NSLS for their contributions to this project. This project is being undertaken at the National Synchrotron Light Source, Brookhaven National Laboratory, which is supported by the US Department of Energy, Office of Basic Energy Sciences and Division of Materials Sciences under contract No. DE-AC02-8CH10886.

#### 5. References

- [1] P. M. Stefan, S. Krinsky, G. Rakowsky, L. Solomon, D. Lynch, T. Tanabe, H. Kitamura, "Small-Gap Research at the NSLS: Concepts and Results", BNL-65092 January, 1997
- [2] D. Lynch, G. Rakowsky, "Mechanical Design of NSLS Mini-gap Undulator (MGU)", 2nd International Workshop on Mechanical Engineering Design of Synchrotron Radiation Equipment and Instrumentation (MEDSI02), Advanced Photon Source, Argonne National Laboratory, Argonne, Illinois U.S.A., September 5-6, 2002 pp. 346-359
- [3] G. Rakowsky, D. Lynch, E. Blum, S. Krinsky, " NSLS In-Vacuum Undulators and Mini-Beta Straights", Proceedings of the 2001 Particle Accelerator Conference, Chicago, Illinois U.S.A. June, 2001, pp. 2453-2455
- [4] J. M. Ablett, L. E. Berman, C. C. Kao, G. Rakowsky and D. Lynch, "Small-gap insertion-device development at the National Synchrotron Light Source – performance of the new X13 mini-gap undulator", (2004). J. Synchrotron Rad. (2004). **11**, pp. 129–131